Irreversible alterations in the hemoglobin structure affect oxygen binding in human packed red blood cells

Ewa Szczesny-Malysiak[a],[1], Jakub Dybas[a],[1], Aneta Blat[a],[b], Katarzyna Bulat[a], Kamil Kus[a],
Magdalena Kaczmarska[a], Aleksandra Wajda[a],[c], Kamilla Malek[b], Stefan Chlopicki[a],[d],
Katarzyna M. Marzec[a],[*]

[a] Jagiellonian Center for Experimental Therapeutics, Jagiellonian University, 14 Bobrzynskiego St., 30-348 Krakow, Poland
[b] Faculty of Chemistry, Jagiellonian University, 2 Gronostajowa Str., 30-387 Krakow, Poland
[c] Faculty of Materials Science and Ceramics, AGH University of Science and Technology, Mickiewicza 30, 30-059 Krakow, Poland
[d] Chair of Pharmacology, Jagiellonian University Medical College, Grzegorzecka 16, 31-531 Krakow, Poland

ARTICLE INFO

ABSTRACT

The ability of hemoglobin (Hb) to transport respiratory gases is directly linked to its quaternary structure properties and reversible changes between T (tense) and R (relax) state. In this study we demonstrated that packed red blood cells (pRBCs) storage resulted in a gradual increase in the irreversible changes in the secondary and quaternary structures of Hb, with subsequent impairment of the T↔R transition. Such alteration was associated with the presence of irreversibly settled in the relaxed form, quaternary structure of Hb, which we termed R′. On the secondary structure level, disordered protein organization involved formation of β-sheets and a decrease in α-helices related to the aggregation process stabilized by strong intermolecular hydrogen bonding. Compensatory changes in RBCs metabolism launched to preserve reductive microenvironment were disclosed as an activation of nicotinamide adenine dinucleotide phosphate (NADPH) production and increased reduced to oxidized glutathione (GSH/GSSG) ratio. For the first time we showed the relationship between secondary structure changes and the occurrence of newly discovered R′, which through an artificial increase in oxyhemoglobin level altered Hb ability to bind and release oxygen.

1. Introduction

Hemoglobin (Hb) is a well-known allosteric protein, where the interactions between spatially distant sites of the molecule change its oxygen affinity. More than 95% of adult Hb is a tetramer called Hb A, consisting of two α and two β similarly sized globin chains ($\alpha_2\beta_2$) [1]. The secondary structure of Hb is represented mainly by α-helices in both α and β globin chains [2–4]. The polypeptide chains are held tightly together primarily by hydrophobic interactions and form two identical dimers – $(\alpha\beta)_1$ and $(\alpha\beta)_2$, thus forming the tertiary structure [5]. In contrast, two dimers are mainly stabilized by much weaker polar interactions– ionic and hydrogen bonding, which can be partially broken during oxygenation process [5]. All four subunits are located roughly at the corners of a tetrahedron giving the Hb its quaternary structure [6,7].

The measure of red blood cells (RBCs) functionality is the ability of Hb to bind and release oxygen. Within each Hb subunit there is an incorporated heme group with centrally coordinated iron ion, directly responsible for oxygen binding [8]. The process of oxygenation is controlled allosterically, what is possible due to the structural shape changes of Hb induced by oxygen binding to the iron ion. Binding of the first oxygen to one of four heme molecules initiates changes in the secondary, tertiary and quaternary structures of the entire tetramer. Each subsequent oxygen molecule binds much more efficiently to the iron ion. This phenomenon is related to the fact that due to the relaxation of the Hb molecule the weak interactions between dimers are partially ruptured, facilitating their movement and allowing the crevice on neighboring subunits to enlarge, and thus to increase Hb oxygen affinity [1]. Fully oxygenated Hb (oxyHb) achieves a relaxed (R) quaternary structure, while fully deoxygenated Hb (deoxyHb) is defined by

a tense (T) quaternary structure [9,10]. The main difference between heme structures in the typical T and R forms is the coordination number of the iron ion. In the T state, the iron is five-coordinated whereas the R state is six-coordinated [11]. Not only oxyHb, but also other liganded Hb derivatives correspond to the R structure, regardless of oxidation state and spin state of the iron ion [12]. Impaired transition between the R and T states of Hb has important consequences in the ability of Hb to bind and release oxygen.

Previously, a number of mechanisms regulating the oxygen affinity in RBCs were proposed, including classical regulation by 2,3-diphosphoglycerate (2,3-DPG) [13,14]. As previously reported, increased oxygen affinity in packed RBCs (pRBCs) results from a storage-related decrease in the concentration of 2,3-DPG [14]. Moreover, additional factors such as temperature, pH or partial pressure of CO_2 are known to influence the binding of oxygen to Hb [15]. Some studies suggested a role of ATP, lactic acid, some other anions [16] or NAD [17] as allosteric effectors in the human Hb. It is important to point out that such mechanisms were previously reported. They explained the behavior of structurally unaltered Hb located inside functional RBCs, where the secondary and quaternary structures of Hb allows for a proper transition between the T and R states and backwards. However, indivertible changes in Hb structure observed inside long-time stored pRBCs were never studied, while they may play a crucial role in the regulation of RBCs function. It can be expected that because of the irreversibly impaired Hb structure, the ability to bind and release oxygen will be permanently altered. According to the official guidelines, erythrocytes can be stored in blood banks up to 42 days, but several reports associate adverse post-transfusion outcomes (i.e. postinjury multiorgan failure) with pRBCs advanced storage age [18,19]. Even though modern storage solutions allow to maintain RBC metabolism and prevent membrane loss [20], the impact of prolonged storage on RBC efficacy was addressed previously [21]. It has been shown that transfusion of old, but not out of date blood products may have negative clinical consequences [22]. This issue draws the attention of researchers, so association between the transfusion of relatively older blood, morbidity and mortality has been demonstrated in multiple retrospective studies utilizing various study designs [19,23–29].

In the present study we focused on detection, definition and characterization of irreversible alterations in the Hb structure in pRBCs. The pRBCs samples were studied weekly for eight weeks with use of blood gas analysis (BGA), UV–Vis spectrophotometry, Raman spectroscopy (RS) and Fourier-transform infrared spectroscopy (FTIR) in respect to their oxygen binding properties. Storage time-dependent changes in pRBCs redox status were revealed by means of liquid chromatography mass spectrometry-based targeted metabolomics (LC-MS/MS) and linked with changes in the Hb structure. Our results shed a new light on the alterations in RBCs integrity induced by long-term storage.

2. Results and discussion

2.1. Changes in Hb species – BGA, UV–Vis and RS

As presented in Fig. 1A–C, a time-dependent gradual increase in oxygen saturation accompanied by an increase in oxyHb and a decrease in deoxyHb content in pRBCs was observed during storage period. A specific pattern of time-dependent shifts was also observed for metHb concentration (Fig. 1D). The values of these parameters stand in line with previous reports, and show that oxygen saturation slightly varies between donors in the first week of storage, what may potentially contribute to donor-specific differences in storage lesion development [30].

Fig. 2 presents UV–Vis absorption spectra of the human pRBCs throughout eight weeks of storage. This technique provides information about molecular structure of the iron ion inside heme proteins, basing on the interpretation of the Soret band position, as well as on the number and the positions of less intense Q bands [31–35]. All collected

spectra were characterized by the presence of the Soret band in the region of 417–420 nm, as well as two Q bands, Q_v (543–544 nm) and Q_0 (578–579 nm), indicating low-spin ferric heme species ($_{LS}Hb^{III}$) [31,33]. As revealed by BGA, the majority of $_{LS}Hb^{III}$ adducts was oxyHb which additionally increased with the time of storage. This is also confirmed by UV–Vis continuous Soret band shift (Fig. 2B) from 420 nm (2nd week) through 419 nm (4th week), 418 nm (6th week) to final 417 nm (8th week). Although bags with the pRBCs were properly mixed before sample collection, the concentration of total Hb adducts slightly varied between each week of measurements, as indicated by absorbance of whole spectra variation. To track semi-quantitative increase in oxyHb concentration we calculated the absorbances' ratio of bands at wavelengths typical for oxyHb (417 nm/579 nm, i.e., Soret/Q_0) (Fig. 2C). Since two main components of the mixture are deoxyHb and oxyHb, and as previously reported the Soret band at around 430 nm for deoxyHb is much more intense comparing to Soret at 417 nm typical for oxyHb [31], a decrease in Soret band at 417 nm accompanied by an increase in 579 nm Q_0, would refer to oxyHb increase. These clearly indicate that similarly as BGA results, UV–Vis also shows a continuous progression in oxyHb level with the time of pRBCs storage. After six weeks of storage, the spectrum of pRBCs (red line) exhibited an increase in the Q_{IV} band located at around 494 nm, indicating further changes in equilibrium between various forms of $_{LS}Hb^{III}$ adducts with a ligand different than oxygen in the sixth coordination side of the iron ion. Interestingly, the CT band observed typically at around 630 nm [32,36] was not observed in the UV–Vis profile, indicating a very low level of metHb formation, as showed by the BGA analysis (up to around 1% of metHb at the end of storage).

Fig. 3A presents RS spectra of pRBCs throughout eight weeks of storage. RS is a technique widely used in heme protein studies [31–33,37], where the use of a proper laser excitation and power is extremely important [38] [39,40]. When excitation wavelength is matched to heme electronic transitions, resonance enhancement of the obtained signal is observed what allows detailed investigation of subtle changes within heme moiety, e.g., associated with ligands binding and changes in Hb quaternary structure [32,37,41].

In case of ferric (Fe^{III}) Hb species, ν_4 mode, which is proposed as an oxidation state marker band [41], and assigned to the symmetric pyrrole half-ring vibration, is located around 1380 cm^{-1}, whereas for ferrous (Fe^{II}) adducts is red-shifted to approximately 1360 cm^{-1} [42]. The spin state sensitive modes reflecting a size of the heme cavity – ν_2 and ν_{10} – appear at 1590 and 1640 cm^{-1}, respectively, for the majority of low-spin (LS) Hb species, and are red-shifted for the high-spin (HS) iron ion [43]. When the ν_{10} mode is found at ca. 1640 cm^{-1}, it is an indicator of the bounded sixth ligand, since only the presence of strong-field ligands explains the LS Hb species [43]. Changes in spin and oxidation states of the iron ion also indirectly reflect heme ruffling, its planarity and deformations, that are all connected with the R ↔ T transitions of the Hb quaternary structure and thus RS can be used for their monitoring [44,45].

In the first week of pRBCs storage the RS spectra indicated that a majority of iron ions inside Hb species exists as oxyHb. Our RS measurements revealed the presence of a mixture of bands typical for oxyHb and those indicating the presence of ferrous Hb species that had arisen due to partial photo/thermal-dissociation of oxyHb and laser-stimulated formation of deoxyHb. Population of $_{LS}Hb^{III}$ adducts increased with the time of storage, as indicated by an increase of intensities of ν_4 (1378 cm^{-1}), ν_2 (1590 cm^{-1}) and ν_{10} (1640 cm^{-1}) modes (Fig. 3B). This was additionally visualized by an increase in ν_2/ν_7 and ν_4/ν_7 ratios where ν_7 originates from the symmetric pyrrole deformation mode that represents an overall Hb concentration [33,46] (Fig. 3C). Significant changes occurred in $_{LS}Hb^{III}$ species contribution after four weeks of pRBCs storage. Such an increase was previously reported in the pRBCs and assigned to oxyHb [39]. The appearance of $_{LS}Hb^{III}$ adducts can also be linked to the formation of hemichrome, which is associated with Hb oxidation and RBCs aging [38,47–49] [38].
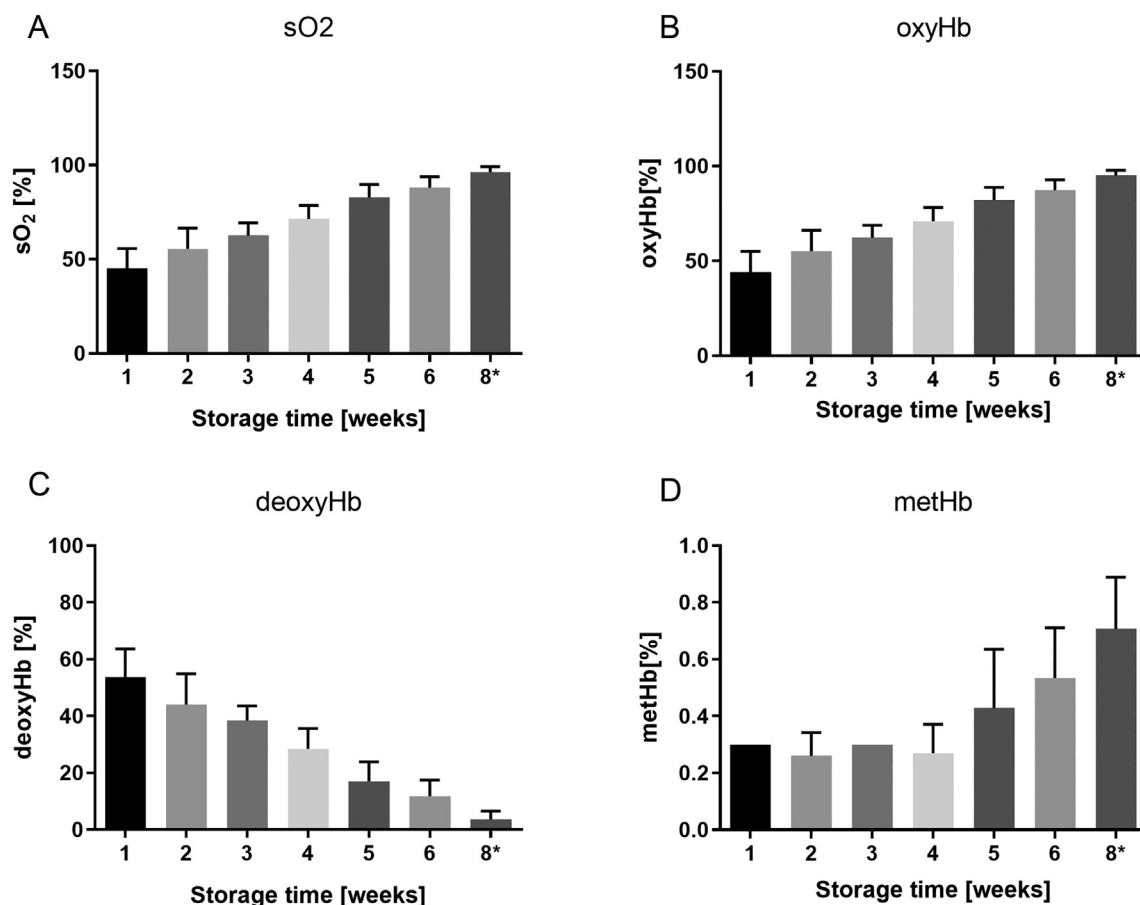
Fig. 1. Time-dependent changes in Hb species in human pRBCs revealed by BGA.

The levels of: (A) oxygen saturation (SO_2), (B) oxyHb, (C) deoxyHb and (D) metHb measured weekly in pRBCs with use of BGA throughout 6 weeks of storage. The data are presented as mean and SD ($N = 10$), blood withdrawn from patients aged 20–39.

*8th week is an additional measurement exceeding expiration date. **The measurements of metHb carried out in weeks 1 and 3 ($N = 5$) gave results of equal values (dataset D).

Altogether, BGA, UV–Vis and RS results revealed that $_{LS}Hb^{III}$ species (mostly present as oxyHb) increased with the time of pRBCs storage. This proves an occurrence of changes in oxygen affinity, resulting from the sum of all alterations appearing in storage conditions, namely a gradual decrease of pH and 2,3-DPG activity, together with an increase in lactate and other RBCs metabolites, what was previously demonstrated [15]. On the other hand, such behavior is non-intuitive because it shows better oxygenation of blood cells that are kept longer in storage. This led to a question, whether pRBCs stored for a longer time could provide more oxygen to cells after transfusion. As we prove further on, at least a part of such increase in oxyHb was related to the gradual and irreversible alterations of the secondary and quaternary structure of Hb. Despite greater oxygenation and oxyHb level, such cells will not be efficient oxygen transporters.

2.2. Irreversible alterations in the secondary structure of Hb in pRBCs correlated to changes in the Hb quaternary structure

It is known that RBCs' proteins comprise an extremely complex mixture of molecules present in the membrane plasma (integral and peripheral proteins) [50], membrane skeleton (spectrin, ankyrin, actin) [51] and in the cytoplasm (90–98% of Hb) [52]. Thus, FTIR features of proteins in RBCs extracted from pRBCs give an averaged information derived from all proteins present in the erythrocytes, with the main contribution of Hb [2,53,54]. Even though Raman spectroscopy can also be used for protein secondary structure examination by analysis of amide I or III located at around 1660 cm^{-1} and 1450 cm^{-1},

respectively [55] such approach is not suitable in case of RBCs studies due to the strong resonance/pre-resonance Raman effect of hemoglobin and enhancement of the heme modes alone [31]. As we have previously reported, semi-quantitative examination of secondary structure of hemoglobin-containing samples was problematic even with the application of 1064 nm excitation wavelength, which is far from resonance conditions [54]. Therefore, to examine secondary protein structure changes within pRBCs during storage-related alterations we employed FTIR spectroscopy [45,56,57]. The studied FTIR spectra region exhibited the presence of amide I (assigned to the stretching vibrations of the C=O groups, with a minor contribution of the C−N stretching and N−H in-plane bending modes) and amide II bands (attributed mainly to the in-plane bending vibration of the N−H bonds and the C−N stretches). Location of amide I bands at 1680, 1660, 1652, 1638, 1629, and 1619 cm^{-1} indicated the presence of intramolecular aggregates, turns, α-helices, unordered structure, β-sheets and intermolecular aggregates, respectively, while amide II bands at 1542 and 1511 cm^{-1} were assigned to α-helical and β-sheet conformations, respectively [58]. Fig. 4 displays second derivative FTIR spectra of pRBCs of three chosen donors (A, B, and C), acquired during the first and sixth week of storage in the spectral range of 1700–1500 cm^{-1}, while spectra collected at other time points, as well as a detailed analysis of intensities of Amide I bands and their correlations are showed in Figs. S1–3.

As revealed in Figs. 4D–F and S2, changes in the intensity ratio of 1629 and 1652 cm^{-1} bands were clearly observed and suggested storage-related imbalance between β-sheets and α-helices in pRBCs. A detailed analysis of band intensities revealed that the band at
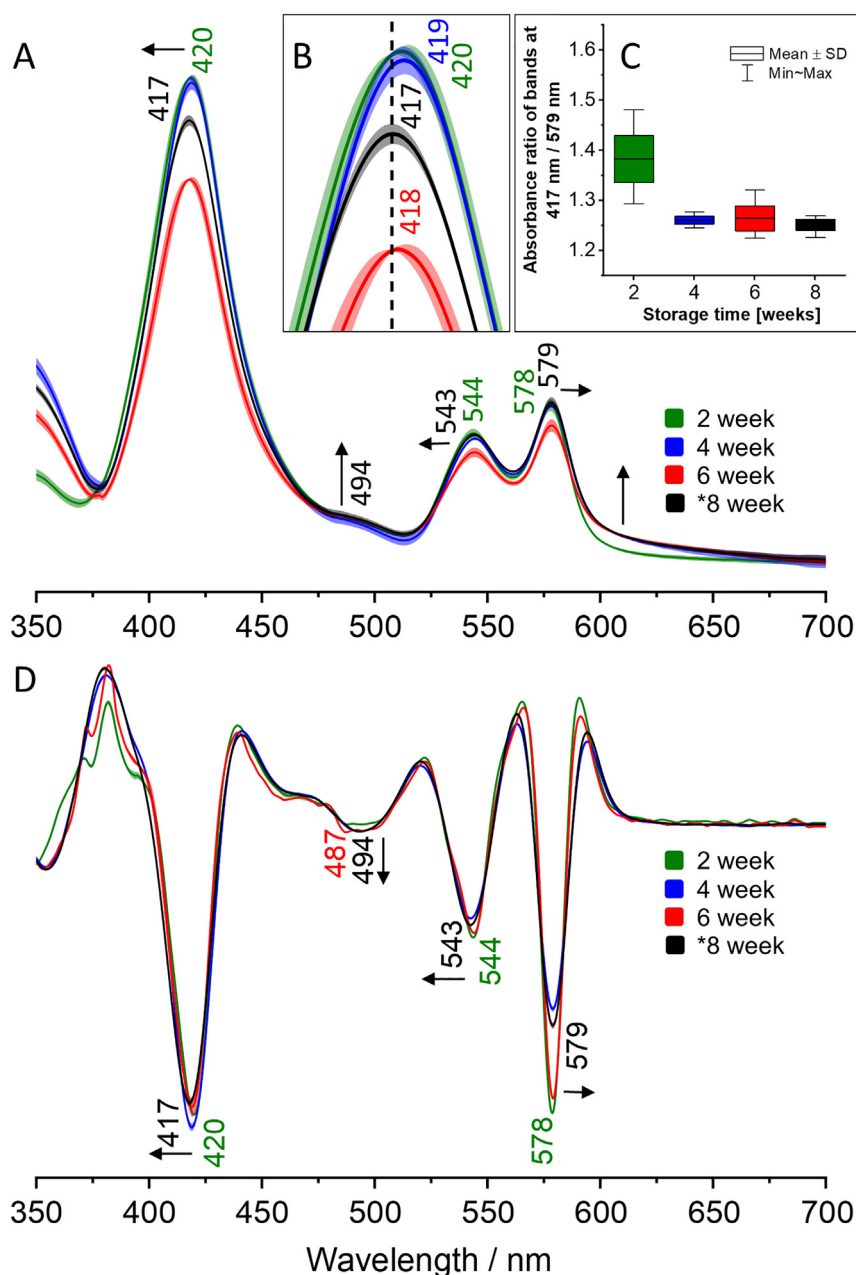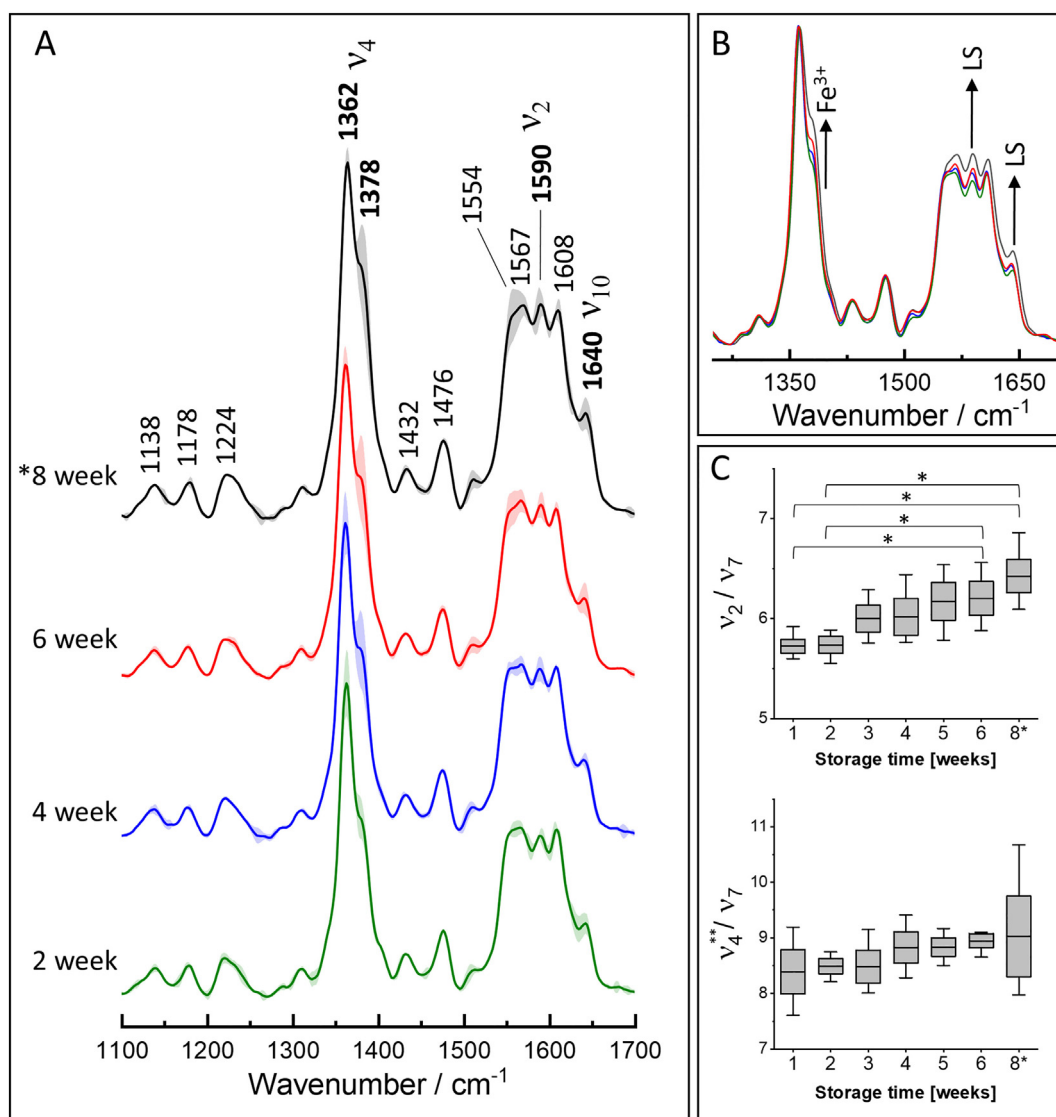
Fig. 2. Time-dependent changes in Hb species in human pRBCs revealed by UV–Vis absorption spectroscopy. (A) Averaged spectra of the human pRBCs stored for 8 weeks ($N = 3$) presented with standard deviation (SD). (B) The inset presents the magnification of 410–430 nm spectral range, highlighting the shift of the Soret band throughout the experimental timeline. (C) The box chart shows a representation of absorbance ratio at 417/579 nm (Soret/Q_0 band), the box corresponds to SD, the line represents mean value and whiskers minimal and maximal values. (D) Second derivatives of the averaged UV–Vis spectra proving the band shifts and lack of variation in baseline between examined samples.

1652 cm^{-1} was the most intense at the beginning of storage period, indicating that Hb inside RBCs existed in α-helix-rich conformation. With the time of storage, absorbance of the β-sheet band increased together with the β-sheet/α-helix ratio, suggesting that α-helix conformation converted into β-sheet. Disappearance of the 1660 cm^{-1} band showed that turn regions in proteins also play a role in secondary structure transformations. Moreover, an increase in the intensity of the 1638 cm^{-1} band disclosed the contribution of unordered structures to this process [58]. Furthermore, changes observed for β-sheets are congruent with intensity changes of the amide I band at 1619 cm^{-1} assigned exclusively to intermolecular interactions between peptide bonds (Figs. S2, 3). Interestingly, intramolecular interactions (revealed by changes in the band at 1680 cm^{-1} [58,59]) weakened in the first two-three weeks of storage, suggesting initial unfolding of proteins. Afterwards they increased reaching the level observed in the first week of storage, this time indicating stiffening of the protein in a new spatial arrangement (Figs. S2, 3). Changes in Hb, including formation of β-sheets accompanied by a decrease in α-helices, indicating an

aggregation process stabilized by strong intermolecular hydrogen bonding, were previously reported for inclusion bodies, folding aggregates, and thermal aggregates [60] as well as Hb interactions with silver ions [58].

Our finding clearly proves the appearance of progressive changes in the secondary structure of Hb in pRBCs and an overall picture of these alterations is presented as the β-sheet/α-helix ratio (Fig. 4D–F). This modification of the secondary structure in the erythrocytes was compared with changes in the quaternary structure determined by BGA for three donors (A, B, and C), where donor-dependent differences in storage lesion development were observed (Fig. 4G–I). In case of donor A, the majority of Hb inside pRBCs was transformed into the R state (oxyHb) in the third week of storage, whereas β-sheets to α-helices ratio started to increase almost from the beginning of storage and remained constant until the end of the investigated period (Fig. 4D and G). This proved exceptional and strong changes in Hb molecular structure in donor A, suggesting that conversion of α-helices into β-sheets induced the formation of irreversibly relaxed state. On the other hand, as

Fig. 3. Time-dependent changes in Hb species in human pRBCs revealed by Raman Spectroscopy. (A) The average RS spectra of the human pRBCs ($N = 3$) obtained from at least 10 single spectra measured weekly with the 488 nm excitation in the region of 1100–1700 cm^{-1} and (B) in the region of 1275–1675 cm^{-1}; (C) box charts represent an increase in $_{LS}Hb^{III}$ adducts with the time of storage, presenting a mean value with SD and whiskers from minimum to maximum values of the integral intensity ratios of ν_2 (spin state marker band, 1580–1600 cm^{-1}) and $\nu_4{**}$ (oxidation state marker band, 1370–1400 cm^{-1} – region typical only for Fe^{III} species) to ν_7 (heme marker band, 740–775 cm^{-1}) mode. Statistical significance was calculated with one-way ANOVA, $*p < 0.05$.

showed in donors B and C, most of the studied pRBCs exhibited a gradual increase in β-sheet to α-helix ratio in the course of the entire storage time. The largest change observed between the fifth and sixth week was accompanied by a similar rate of oxyHb generation (Fig. 4E, F and H–I). Interestingly, in the time point exceeding expiration date (week 8) oxyHb content reached ca. 95%, whereas changes in the secondary structure suddenly dropped down to the level observed in the first week. As UV–Vis absorption indicated, this fact most likely resulted from a massive hemolysis leading to a release of Hb from RBCs and an extensive degradation of the Hb secondary structure.

The combination of FTIR and BGA results indicated that conversion into oxyHb is preceded by irreversible changes in the secondary structure of Hb. This may also suggest that the changes in quaternary structure manifested by oxyHb increase, are irreversible.

2.3. Irreversible alterations in the quaternary structure of Hb in pRBCs

As previously reported [61], repeated treatment of the RBCs with sodium dithionate evokes an increase in oxygen uptake with each subsequent dose. This was previously explained by increased formation of the R state after each addition of sodium dithionate, due to an impairment of the quaternary structure of Hb [61]. In the experiment presented in Fig. 5 we have compared the results of three subsequent sodium dithionate treatments on a set of pRBCs in the first ($N = 3$) and fifth (N = 3) week of storage using UV–Vis absorption spectroscopy. Each dose of sodium dithionite induced the conversion of oxyHb to deoxyHb and then the spontaneous recovery in the air to oxyHb form (T → R). The rate of conversion (min) was monitored by changes in the position of the Soret band (from around 434 nm – typical for deoxyHb to around 418 nm – typical for oxyHb) and recorded for three individual samples (N = 3, Fig. 5A). For the comparison we chose the fifth week, since the biggest changes in the Hb secondary structure in pRBCs were observed in the fifth/sixth week of storage (Fig. 4). This indicates the impact of changes in the secondary structure on the functioning of the quaternary Hb structure and formation of R′ structure inside altered RBCs. It was previously reported that pRBCs stored for at least 3 weeks are characterized by impaired oxygen uptake and release [62], what was postulated to be related with changes in 2,3-DPG
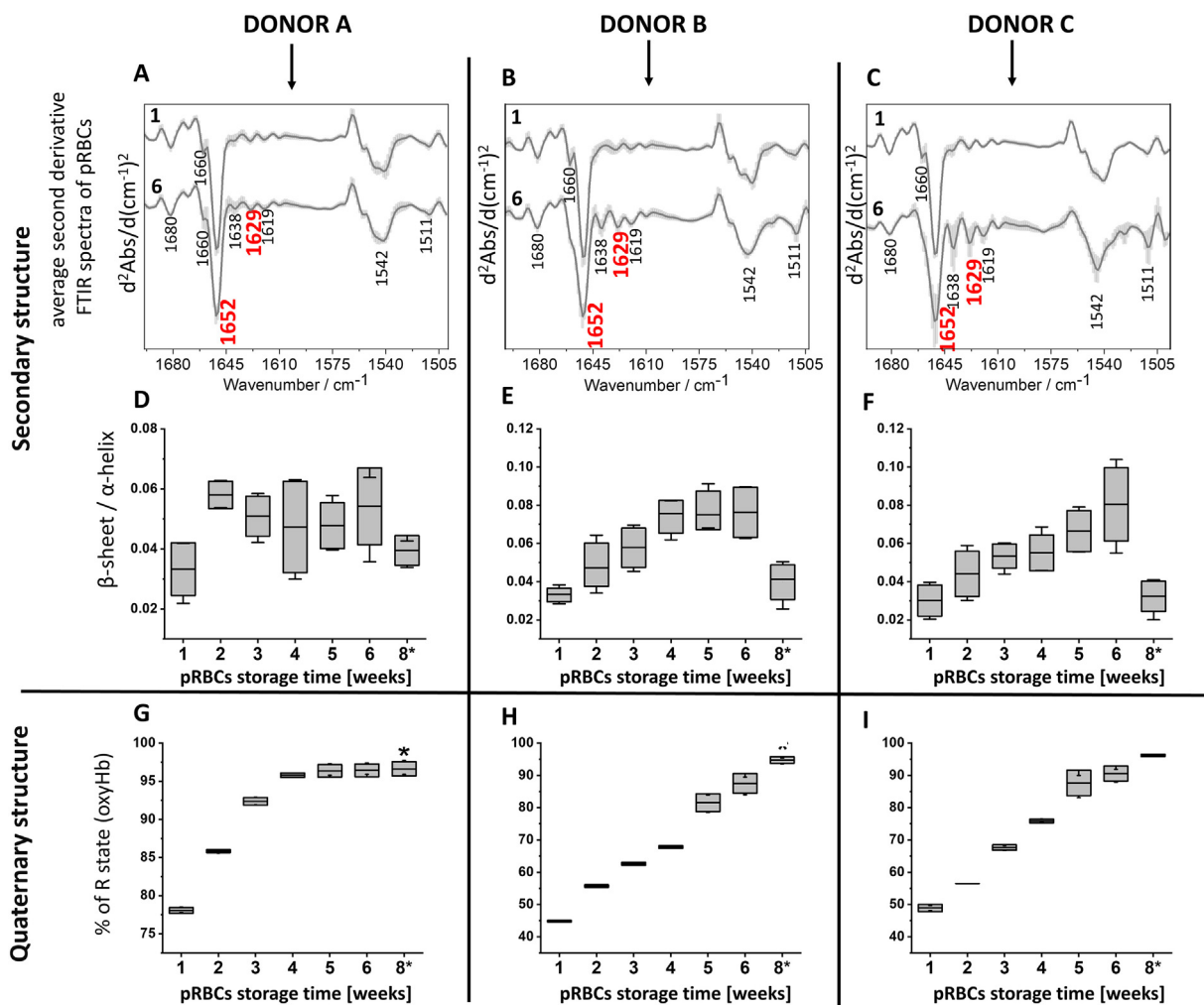
Fig. 4. Time-dependent changes in Hb secondary structure in human pRBCs revealed by FTIR. (A–C) Second derivative FTIR spectra of the pure RBC fraction of pRBCs collected after the first and sixth week of storage for different blood donors (A, B, C) with the (D–F) ratio of integral intensities of the bands at 1629 cm^{-1} and 1652 cm^{-1} corresponding to β-sheets/α-helices ratio showing the alterations in secondary structures of RBCs. The integration regions for IR bands: at 1652 cm^{-1} (1665–1642 cm^{-1}) and at 1629 cm^{-1} (1633–1624 cm^{-1}); (G–I) the levels of oxyHb for donors A, B, C measured weekly in pRBCs with use of BGA. All data are presented as mean and SD for blood withdrawn from patients aged 20–39. *8th week is an additional measurement exceeding expiration date.
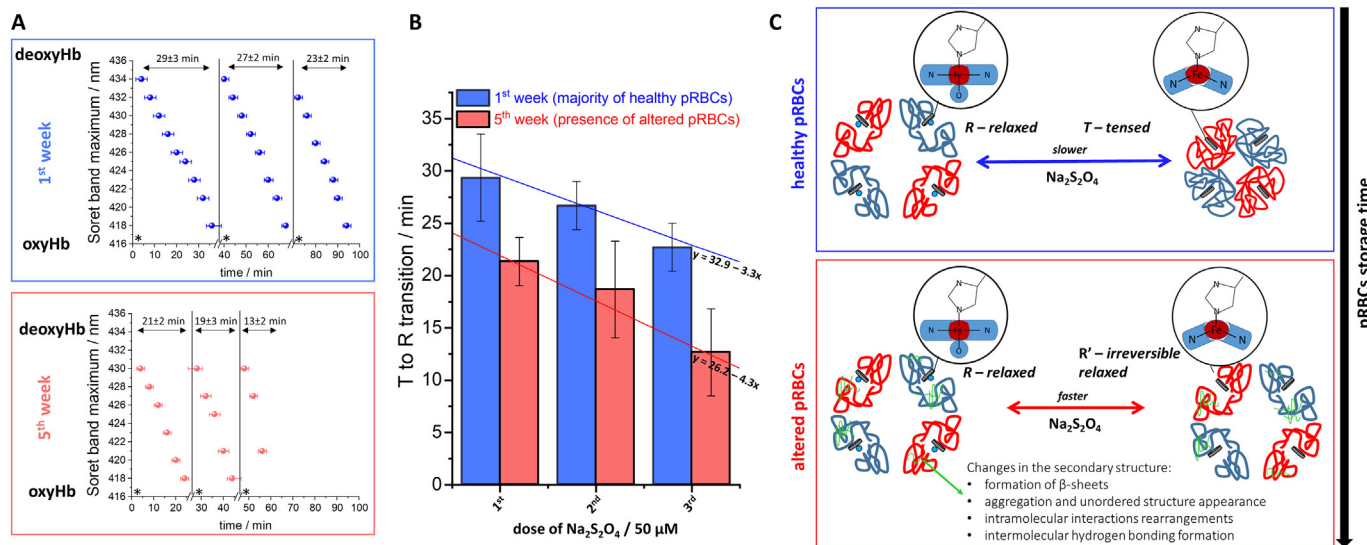
Fig. 5. (A) Comparison of time of the transition between T (deoxyHb) to R (oxyHb) state after three subsequent sodium dithionate treatments on a set of pRBCs in the first (N = 3) and fifth (N = 3) week of storage using UV–Vis absorption spectroscopy. (B) The average times of T → R transitions with calculated rate of T → R conversion (C) schematic illustration of T → R transition evoked by sodium dithionate administration (upper panel) and visualization of R′ formation (lower panel).

level. However, as indicated by our results presented in Fig. 5 obtained from highly diluted (1:1000) pRBCs suspended in the saline solution, such change is mainly associated with alterations in molecular structure of Hb rather than microenvironment variations of RBCs including pH, temperature or 2,3-DPG concentration.

These results clearly revealed that in the first week of pRBCs storage, T to R state transition (T → R, transition from deoxyHb to oxyHb) required longer period of time (around 30 min) after the first dose of sodium dithionate, as compared with pRBCs in the fifth week of storage (around 20 min). Similarly, the comparison of regression line slopes of the average time between T → R state transition (Fig. 5B) obtained for repeated doses of sodium dithionate in the first and fifth week showed much faster process of T → R in the fifth week of pRBCs storage (the slope is more steep).

This suggest the presence of the higher level of irreversibly altered quaternary structure of Hb in the fifth week of pRBCs storage, and therefore much faster oxygen uptake than in the first week (presented schematically in Fig. 5C). Such faster oxygen uptake seems enabled due to the presence of irreversible, quaternary structure of Hb, stiffened in the relaxed form, which we termed R′. We hypothesize that the R′ form has no ligand in the sixth coordination site of Hb after addition of sodium dithionate, but does not shape-shift to the proper T state on the level of quaternary structure. The existence of Hb preserved in the R′ state is also supported by FTIR-proven conversion of the dominant rigid α-helix into β-sheet structure, as well as by the increase in stronger intermolecular interactions that suggest aggregation on the level of secondary Hb structure, which also makes quaternary structure more rigid and inflexible. The R′ → R conformational change is connected with oxygen binding, while the T → R transformation is related to the change between tense and relaxed state of the quaternary Hb structure during binding of oxygen molecule. In case of altered quaternary structure of Hb in the fifth week of pRBCs storage, the T → R transfer should be presented as T/R′ → R. In such condition, typical structural shape changes of Hb induced by oxygen binding to the iron ion are disrupted. In healthy RBCs where the quaternary structure is not altered, the proper, longer and allosterically controlled T → R transition takes place and allows for a gradual admission or release of oxygen molecules. The presence of the R′ state inside RBCs results in faster oxygen uptake and release without the proper transition to the T form on the level of quaternary structure of Hb. Thus, the presence of R′ excludes the slow and gradual release of oxygen molecules, what can be problematic in case of oxygen transport to microcirculation. Moreover, since it is known that sodium dithionate addition itself causes alterations in the quaternary Hb structure [61], we may conclude, that RBCs with R′ are more sensitive to additional adverse factors, i.e., every subsequent dose of dithionate.

2.4. Effects of pRBCs storage on intracellular redox state

To analyze the impact of the storage time on pRBCs redox state, levels of reduced glutathione (GSH) and oxidized glutathione (GSSG) were measured. Subsequently, GSH/GSSG ratio was calculated, in order to characterize RBCs antioxidative activity. As shown in Fig. 6A, the level of reduced form of glutathione increases with time. On the other hand, the level of oxidized form of glutathione (GSSG), after an initial increase seen in the first two weeks of storage, decreases gradually (Fig. 6B). Glutathione is one of the most important parts of the antioxidant system found in the erythrocytes. Although other authors reported time-dependent decreases in GSH levels in stored RBCs [63,64], initial amounts of GSH inside RBCs reported in our study were lower than those reported by others. It is well known that GSH readily oxidizes non-enzymatically and that biological samples are acidified quickly to reduce oxidation of GSH to GSSG and to mixed disulfides. [65] Our results revealed an increase in GSH and a two-phase response of GSSG, including an increase and then a decrease, progressing with the time of storage. The progressive increase of the GSH/GSSG ratio

(Fig. 6C) suggests the shift of the metabolism inside pRBCs as a response to oxidative cellular microenvironment.

Erythrocytes are capable of synthesizing glutathione from L-cysteine (homocysteine being its precursor), glutamate and glycine [66] but we did not observe a decrease in the levels of any of the required aminoacids – neither in the RBCs fraction, nor in the SAGM solution supernatant (Fig. S4). In fact, an increase in homocysteine may reflect increased activation of GSH synthesis. Moreover, no active transport of GSSG out of the RBCs was detected, because we did not see any increase of GSSG levels in the supernatant (Fig. S5).

It also has to be mentioned, that because of lactate accumulation accompanied by a decrease in glucose concentration (Fig. S6), pRBCs environment was distinctly acidic (pH was decreasing gradually reaching the value below 6 in the third week of storage; data not shown), what prevented GSH oxidation and additionally supported lack of GSSG increase [65].

Since oxidized form of glutathione is potentially toxic to the cells, RBCs maintain high glutathione reductase (GSSGR) activity for efficient conversion of GSSG to GSH [66]. The action of GSSGR depends on NADPH [67] and erythrocytes convert NADP to NADPH exclusively in the pentose phosphate pathway (PPP) to maintain high GSH levels [68]. Our results suggest that NAPDH is largely preserved even throughout eight weeks storage with a transient but significant increase in the second week, while PPP metabolites display a progressive increase (Fig. 6D–F), suggesting an activation of PPP that facilitates regeneration of GSH pool. These metabolomic results suggests that pRBCs storage resulted in changes of metabolism directed to maintain reductive equivalent pool for protection against oxidative stress, as evidenced by activation of PPP-derived NADPH production and increased GSH/GSSG ratio.

3. Summary and conclusions

In this work a systematic study of changes in the secondary and quaternary structures of Hb observed weekly in situ in pRBCs was reported. We correlated the structure of hemoglobin with its oxygen binding properties and changes in pRBCs metabolic state. The combination of BGA, UV–Vis, RS and FTIR spectroscopies allowed for a detailed in situ analysis of irreversible alterations in the secondary and quaternary structures of Hb in functional RBCs during storage of pRBCs. FTIR showed alterations in the Hb secondary structures, where the dominant conversion of α-helices into β-sheets is accompanied by formation of intermolecular interactions and unordered arrangements of the hemoprotein. These conformational changes of Hb co-occured with a gradual increase in oxygen saturation, resulting from the presence of irreversibly relaxed form of quaternary structure of Hb termed R′.

When compared to the first week, a higher level of the R′ state of Hb observed in the fifth week of pRBCs storage cannot be connected with neither the variation of pH, temperature nor any other environmental factor. The information about the presence of R′ was obtained from the experiment where UV–Vis spectra were obtained from highly diluted (1:1000) pRBCs suspended in the saline solution. In such conditions pH, temperature and other factors, e.g. 2,3-DPG do not vary, and therefore observed alterations refer to pRBCs alone (Fig. 5). Storage time-dependent increase in irreversible R′ state of Hb in pRBCs is responsible for an artificial increase in both oxygen uptake and oxyHb concentration. pRBCs containing R′ state-rich Hb are also characterized by faster oxygen uptake and release, when compared to RBCs without R′ Hb. In fact, on the functional level the process of T → R transition (conversion from deoxyHb to oxyHb) was faster after five weeks of pRBCs storage, as it already had adopted the irreversible R′ form. Metabolomic analysis performed with a special regard to GSH/GSSG ratio revealed a gradual increase in GSH/GSSG ratio throughout pRBCs storage. This was accompanied by an initial increase (second week), followed by a gradual decrease in NADPH level. Moreover, we have observed an increase in the levels of pentose phosphate cycle end-products: erytrose-4-
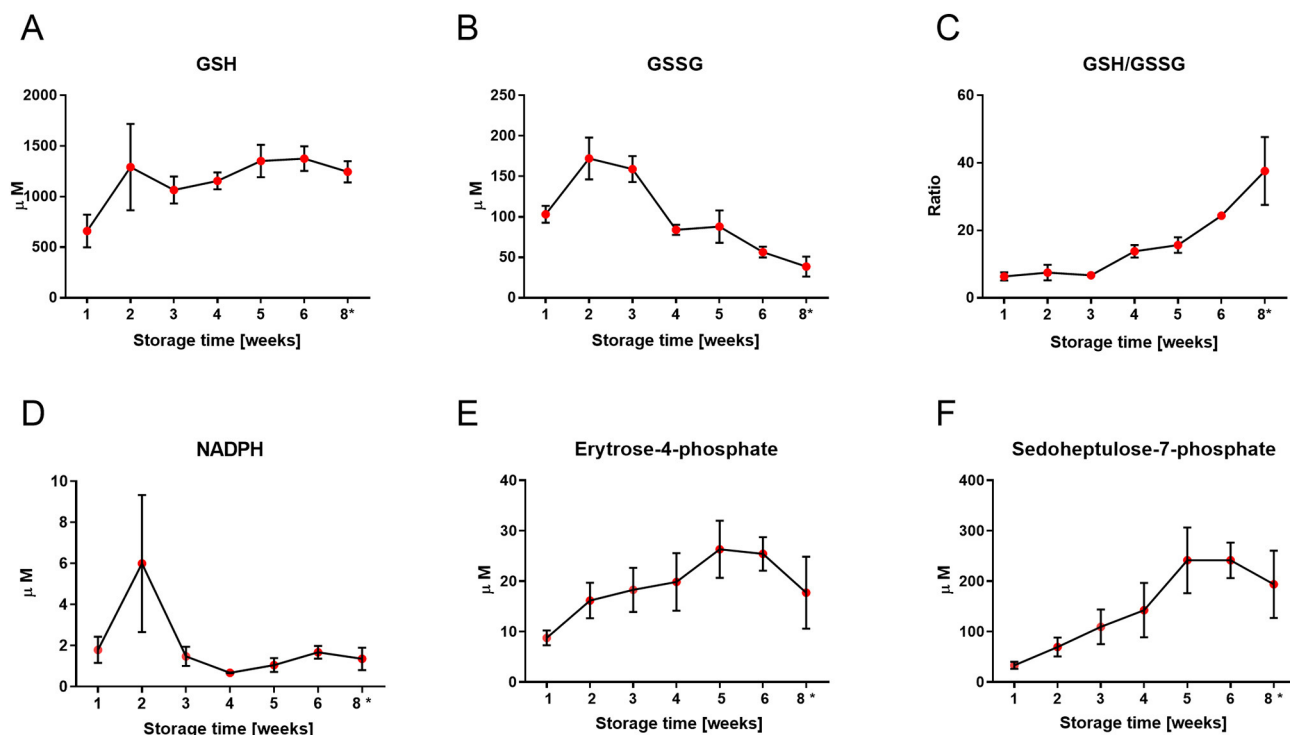
Fig. 6. The impact of storage on the redox state and PPP metabolites in human pRBC.
Changes in different forms of glutathione (GSH) and the pentose phosphate pathway (PPP) measured with use of LC-MS/MS throughout 6 weeks of storage: A) reduced form of glutathione (GSH); B) oxidized form of glutathione (GSSG); C) measure of tissue antioxidative activity (GSH/GSSG); D) NADPH; E) erytrose-4-phosphate; F) sedoheptulose-7-phosphate. The data are presented as mean and SD, blood withdrawn from patients aged 20–29 ($N = 3$), *8th week is an additional measurement exceeding bags' expiration date.

phosphate and sedoheptulose-7-phosphate, what is responsible for maintaining NADPH levels to enable further GSSG reduction, and therefore for the prevention of oxidative stress-related damage. As it is known, low GSH levels reflect pro-oxidant conditions, so it has to be assumed that pRBCs maintained high GSSGR activity, what helped them overcome initial high oxidative stress resulting from blood withdrawal and banking procedure, especially since we did not observe any GSSG increase in the SAGM solution supernatant.

In conclusion, alterations in the secondary Hb structure increase progressively with the time of pRBCs storage and are manifested as formation of β-sheets accompanied by a decrease in α-helices, evoked by the aggregation process stabilized by strong intermolecular hydrogen bonding. This in turn has an impact on the quaternary Hb structure and causes the formation of the R′ quaternary structure of Hb, irreversibly preserved in the relaxed form. The presence of R′ has an impact on T↔R transition and the T/R ratio, what in consequence, affects oxygen uptake and release, and thus impairs oxygen bioavailability. The results of metabolomic analysis did not allow us to conclude about the origin of the irreversible changes observed in the secondary and quaternary structure of Hb during pRBCs storage, however they clearly showed that alterations do not occur due to oxidative stress, but rather are the means to maintain reductive cellular microenvironment. Important physiological consequences of the irreversible Hb structure changes relate to the microcirculation of peripheral tissues, where defective ability for T↔R changes may impair oxygen transport and delivery. However, further studies are required to confirm the impact of transfusion of stored pRBCs with artificially increased level of oxyHb due to the presence of irreversible R′ state on oxygenation status of peripheral tissues in patients.

4. Methods

4.1. Packed red blood cells (pRBCs)

Leukocyto-depleted pRBCs in hermetic blood bags containing SAGM (Saline, Adenine, Glucose, Mannitol) additive solution and a small amount of CPD (Citrate, Phosphate, Dextrose) preservative were purchased from the Regional Centre for Blood Donation and Haemotherapy in Krakow. Informed consent was given by each volunteer prior to the blood withdrawal and the study conformed with the principles outlined in the World Medical Association (WMA) Declaration of Helsinki, as well as a Bioethical Commission of the Jagiellonian University. In this study bags prepared from the whole blood donated by men aged 20–39 were used ($N = 3$ for most applied techniques; $N = 10$ for BGA results). All analyzes were carried out weekly throughout six weeks of pRBCs storage, while the eighth week's measurements were designed as an additional time point exceeding pRBCs' expiration date (42 days). Before each week's measurements, pRBCs were properly mixed.

4.2. Blood gas analysis (BGA)

BGA was carried out for pRBCs with the use of a SIEMENS RAPIDPoint® 500 Analyzer (Siemens AG, Germany), according to the manufacturer's instructions. Each sample was analyzed three times to assess oxygen saturation (sO_2), oxyhemoglobin (oxyHb), methemoglobin (metHb) and deoxyhemoglobin (deoxyHb). The mean and SD were calculated.

4.3. UV–Vis spectrophotometry (UV–Vis)

Absorption spectra were recorded on a Perkin Elmer double beam spectrophotometer Lambda 950 in the range of 350–700 nm using a cuvette of a 1 cm path length. pRBCs samples were diluted 1:1000 (v:v)

with 0.9% NaCl solution.

4.4. Raman spectroscopy (RS)

RS measurements of the functional RBCs fractions obtained from pRBCs were conducted on a WITec confocal CRM alpha 300 Raman microscope with use of 488 nm excitation wavelength. The laser was coupled to the microscope via an optical fiber (50 μm diameter). The water immersive Nikon Fluor (60×/1.00 NA) objective was used. Spectral resolution was equal to 3 cm^{-1}. The monochromator of the spectrometer was calibrated using radiation spectrum from a xenon lamp (WITec UV–light source). Additionally, standard alignment procedure (single-point calibration) was performed before collection of spectra with use of Raman scattering line produced by a silicon plate (520.5 cm^{-1}).

To collect the spectra from pRBCs, we applied a 488 nm excitation wavelength laser with the power of 100 μW in the focus spot. A size of the laser spot was around 0.6 μm in diameter (size of the laser spot = 1.22λ / NA, where λ is the wavelength of the laser and NA is the numerical aperture of the used objective). Applied experimental conditions were a compromise to obtain good signal-to-noise ratio from a single measurement and the presence of partial photo/thermal-dissociation of bounded ligands. This methodology was maintained during all the measurements, what allowed us to conclude about overall changes in Hb species during storage.

Pure RBCs fraction samples were diluted 1:1000 (v:v) with PBS without ions solution and transferred into a glass bottom dish with a CaF_2 window on the bottom. When the RBCs formed the monolayer on the CaF_2 slide, Raman spectra were collected from at least ten randomly chosen spots. Estimated acquisition time was 60 s (20 accumulations, 3 s integration time). Laser power in the focus spot was equal to 100 μW. Data collection and analysis were performed using WITec (WITec Project Plus 5), Opus 7.2, and OriginPro 2018 programs.

4.5. Fourier transform infrared spectroscopy (FTIR)

FTIR spectra were collected for the pure fraction of RBCs (obtained from pRBCs) using a Bruker Alpha FTIR spectrometer equipped with a single-bounce diamond ATR crystal. Spectra were acquired with a 4 cm^{-1} spectral resolution in the range of 3800–900 cm^{-1} by co-adding 64 scans. 1.5 μl of RBCs were deposited onto the ATR crystal and air-dried for 5 min in room temperature. Each spectrum was recorded for approximately 2 min. The background of the clean ATR crystal was recorded before each measurement. Five replicates for each sample were collected.

FTIR spectra were preprocessed and analyzed with OPUS and Origin 2018 Pro software. All spectra were vector normalized in the region from 900 to 1461 cm^{-1}. All spectra for a given sample were averaged and SD was calculated. Integral intensities of the selected bands were calculated as a band area and the box charts of bands intensities were constructed to show their average value with SD and min-max value.

4.6. Liquid chromatography-mass spectrometry (LC-MS/MS) and metabolomics

Detection of intracellular metabolites was performed according to the protocol described previously [69], with minor changes. Briefly, an aliquot of 50 μl of pRBCs was centrifuged (500 $\times g$, 10 min, RT, no braking) and divided into two fractions – pure fraction of RBCs (RBCs fraction) and SAGM solution supernatant. Intracellular metabolites from RBC fraction were extracted with 0.5 ml of dry-ice-cold extraction solution (acetonitrile: methanol: water 5:2:3, v/v/v), lyophilized and reconstituted in 30 μl of MS-grade water.

A volume of 5 μl of each sample was injected into LC column and analyzed on QTRAP 5500 (Sciex, Framingham, MA, USA) coupled with UFLC Nexera (Shimadzu, Kyoto, Japan). Chromatography separation

was performed with use of Acquity UPLC BEH C18 1.7 μm 3.0 × 150 mm analytical column (Waters, Milford, MA, USA) using acetonitrile: 100 mM ammonium acetate (pH 5.8) 95:5 v/v and 5 mM ammonium acetate (pH 5.8) as a mobile phase in gradient elution. Samples were analyzed twice- in positive and negative ionization MRM mode. The ion source operation conditions were: Curtain Gas: 25 psi, Collision Gas: medium, Temperature: 500 °C, Ion Source Gas 1: 40 arb., Ion Source Gas 2: 50 arb. and IonSpray Voltage: 5500 V and −4500 V for positive and negative ionization modes, respectively.

CRediT authorship contribution statement

Ewa Szczesny-Malysiak: Formal analysis, Data curation, Writing - original draft.**Jakub Dybas:**Investigation, Formal analysis, Data curation, Writing - original draft.**Aneta Blat:**Investigation, Formal analysis.**Katarzyna Bulat:**Investigation, Formal analysis.**Kamil Kus:**Investigation.**Magdalena Kaczmarska:**Resources, Formal analysis, Investigation.**Aleksandra Wajda:**Resources, Formal analysis, Investigation.**Kamilla Malek:**Formal analysis, Data curation.**Stefan Chlopicki:**Writing - review & editing.**Katarzyna M. Marzec:**Conceptualization, Methodology, Writing - original draft, Writing - review & editing.

Declaration of competing interest

The authors declare that they have no known competing financial interests or personal relationships that could have appeared to influence the work reported in this paper.

Appendix A. Supplementary data

Supplementary data to this article can be found online at https://doi.org/10.1016/j.bbamcr.2020.118803.

References

[1] C. Thomas, A.B. Lumb, Physiology of haemoglobin, Contin. Educ. Anaesthesia, Crit. Care Pain. 12 (2012) 251–256. https://doi.org/10.1093/bjaceaccp/mks025.

[2] P. Prevelige, G.D. Fasman, Chou-Fasman Prediction of the Secondary Structure of Proteins BT - Prediction of Protein Structure and the Principles of Protein Conformation, in: G.D. Fasman (Ed.), Springer US, MA, Boston, 1989, pp. 391–416, , https://doi.org/10.1007/978-1-4613-1571-1_9.

[3] W.L. Nichols, B.H. Zimm, L.F. Ten Eyck, Conformation-invariant structures of the α1β1 human hemoglobin dimer11Edited by P. E. Wright, J. Mol. Biol. 270 (1997) 598–615. https://doi.org/10.1006/jmbi.1997.1087.

[4] A.H. Hegde, B. Sandhya, J. Seetharamappa, Investigations to reveal the nature of interactions of human hemoglobin with curcumin using optical techniques, Int. J. Biol. Macromol. 52 (2013) 133–138, https://doi.org/10.1016/J.IJBIOMAC.2012.09.015.

[5] R.A. Harvey, D.R. Ferrier, Lippincott's Illustrated Reviews: Biochemistry Fifth Edition, 5th ed., Wolters Kluwer, Lippincott Williams and Wilkins, Baltimore, Philadelphia, 2011.

[6] J. Old, Hemoglobinopathies and thalassemias, in: Emery Rimoin's Princ. Pract. Med. Genet., 2013: pp. 1–44. https://doi.org/10.1016/B978-0-12-383834-6.00075-6.

[7] G.A. Petsko, D. Ringe, Protein structure and function, Protein Struct. Funct, Elsevier, 2004, p. 195, , https://doi.org/10.1021/ja209464f.

[8] K. Kaushansky, M.A. Lichtman, J.T. Prchal, M.M. Levi, O.W. Press, L.J. Burns, M.A. Caligiuri, Hematology, 9th ed., New York Chicago San Francisco Athens London Madrid Mexico City Milan New Delhi Singapore Sydney Toronto, 2016.

[9] M.K. Safo, M.H. Ahmed, M.S. Ghatge, T. Boyiri, Hemoglobin-ligand binding: understanding Hb function and allostery on atomic level, Biochim. Biophys. Acta - Proteins Proteomics. 1814 (2011) 797–809, https://doi.org/10.1016/j.bbapap.2011.02.013.

[10] N. Shibayama, S. Saigo, Direct observation of two distinct affinity conformations in

the T state human deoxyhemoglobin, FEBS Lett. 492 (2001) 50–53, https://doi.org/10.1016/S0014-5793(01)02225-6.

[11] M.F. Perutz, Regulation of oxygen affinity of hemoglobin: influence of structure of the globin on the heme iron, Annu. Rev. Biochem. 48 (1979) 327–386, https://doi.org/10.1146/annurev.bi.48.070179.001551.

[12] N. Shibayama, Allosteric transitions in hemoglobin revisited, Biochim. Biophys. Acta - Gen. Subj. 2020 (1864), https://doi.org/10.1016/j.bbagen.2019.03.021.

[13] R. Benesch, R.E. Benesch, The effect of organic phosphates from the human erythrocyte on the allosteric properties of hemoglobin, Biochem. Biophys. Res. Commun. 26 (1967) 162–167, https://doi.org/10.1016/0006-291X(67)90228-8.

[14] R. Macdonald, Red cell 2,3-diphosphoglycerate and oxygen affinity, Anaesthesia. 32 (1977) 544–553, https://doi.org/10.1111/j.1365-2044.1977.tb10002.x.

[15] R.N. Pittman, Chapter 4, oxygen transport, Regul. Tissue Oxyg. 2011.

[16] J. Celia, Bonaventura, competition in oxygen-linked anion binding to normal and variant human hemoglobins, Hemoglobin 4 (1980) 275–289, https://doi.org/10.3109/03630268008996210.

[17] R. Cashon, C. Bonaventura, J. Bonaventura, A. Focesi, The nicotinamide adenine dinucleotides as allosteric effectors of human hemoglobin, J. Biol. Chem. 261 (1986) 12700–12705.

[18] W.L. Biffl, E.E. Moore, P.J. Offner, D.J. Ciesla, R.J. Gonzalez, C.C. Silliman, Plasma from aged stored red blood cells delays neutrophil apoptosis and primes for cytotoxicity: abrogation by poststorage washing but not prestorage leukoreduction, J. Trauma - Inj. Infect. Crit. Care, Lippincott Williams and Wilkins, 2001, pp. 426–432, , https://doi.org/10.1097/00005373-200103000-00005.

[19] G. Zallen, P.J. Offner, E.E. Moore, J. Blackwell, D.J. Ciesla, J. Gabriel, C. Denny, C.C. Silliman, Age of transfused blood is an independent risk factor for postinjury multiple organ failure, Am. J. Surg. 178 (1999) 570–572, https://doi.org/10.1016/S0002-9610(99)00239-1.

[20] J.R. Hess, An update on solutions for red cell storage, Vox Sang. 91 (2006) 13–19, https://doi.org/10.1111/j.1423-0410.2006.00778.x.

[21] E. Almac, C. Ince, The impact of storage on red cell function in blood transfusion, Best Pract. Res. Clin. Anaesthesiol. 21 (2007) 195–208 (http://www.ncbi.nlm.nih.gov/pubmed/17650772 (accessed September 11, 2011)).

[22] M.J. Vandromme, G. McGwin, J.A. Weinberg, Blood transfusion in the critically ill: Does storage age matter?, Scand. J. Trauma. Resusc. Emerg. Med. 17 (2009). https://doi.org/10.1186/1757-7241-17-35.

[23] M.E. Keller, R. Jean, W.W. LaMorte, F. Millham, E. Hirsch, Effects of age of transfused blood on length of stay in trauma patients: a preliminary report, J. Trauma 53 (2002) 1023–1025, https://doi.org/10.1097/01.TA.0000031178.15943.18.

[24] C.G. Koch, L. Li, D.I. Sessler, P. Figueroa, G.A. Hoeltge, T. Mihaljevic, E.H. Blackstone, Duration of red-cell storage and complications after cardiac surgery, N. Engl. J. Med. 358 (2008) 1229–1239, https://doi.org/10.1056/NEJMoa070403.

[25] P.J. Offner, E.E. Moore, W.L. Biffl, J.L. Johnson, C.C. Silliman, Increased rate of infection associated with transfusion of old blood after severe injury, Arch. Surg. 137 (2002) 711–716 (discussion 716-7. http://www.ncbi.nlm.nih.gov/pubmed/12049543 (accessed September 11, 2016)).

[26] F.R. Purdy, M.G. Tweeddale, P.M. Merrick, Association of mortality with age of blood transfused in septic ICU patients, Can. J. Anaesth. 44 (1997) 1256–1261, https://doi.org/10.1007/BF03012772.

[27] E.C. Vamvakas, J.H. Carven, Transfusion and postoperative pneumonia in coronary artery bypass graft surgery: effect of the length of storage of transfused red cells, Transfusion. 39 (1999) 701–710 (http://www.ncbi.nlm.nih.gov/pubmed/10413277 (accessed September 11, 2016)).

[28] J.A. Weinberg, G. McGwin, M.B. Marques, S.A. Cherry, D.A. Reiff, J.D. Kerby, L.W. Rue, Transfusions in the less severely injured: does age of transfused blood affect outcomes? J. Trauma - Inj. Infect. Crit. Care. 65 (2008) 794–798, https://doi.org/10.1097/TA.0b013e318184aa11.

[29] J.A. Weinberg, G. McGwin, R.L. Griffin, V.Q. Huynh, S.A. Cherry, M.B. Marques, D.A. Reiff, J.D. Kerby, L.W. Rue, Age of transfused blood: an independent predictor of mortality despite universal leukoreduction, J. Trauma 65 (2008) 279–282 discussion 282-4 https://doi.org/10.1097/TA.0b013e31817c9687.

[30] T. Yoshida, A. Blair, A. D'alessandro, T. Nemkov, M. Dioguardi, C.C. Silliman, A. Dunham, Enhancing uniformity and overall quality of red cell concentrate with anaerobic storage, Blood Transfus. 15 (2017) 172–181, https://doi.org/10.2450/2017.0325-16.

[31] K.M. Marzec, D. Perez-Guaita, M. de Veij, D. McNaughton, M. Baranska, M.W. a. Dixon, L. Tilley, B.R. Wood, Red blood cells polarize green laser light revealing hemoglobin's enhanced non-fundamental Raman modes, ChemPhysChem. 15 (2014) 3963–3968. https://doi.org/10.1002/cphc.201402598.

[32] K.M. Marzec, J. Dybas, S. Chlopicki, M. Baranska, Resonance raman in vitro detection and differentiation of the nitrite-induced hemoglobin adducts in functional human red blood cells, J. Phys. Chem. B 120 (2016) 12249–12260, https://doi.org/10.1021/acs.jpcb.6b08359.

[33] J. Dybas, P. Berkowicz, B. Proniewski, K. Dziedzic-Kocurek, J. Stanek, M. Baranska, S. Chlopicki, K.M. Marzec, Spectroscopy-based characterization of Hb–NO adducts in human red blood cells exposed to NO-donor and endothelium-derived NO, Analyst 143 (2018) 4335–4346, https://doi.org/10.1039/C8AN00302E.

[34] C. Lu, T. Egawa, M. Mukai, S.-R. Yeh, Hemoglobins from Mycobacterium tuberculosis and Campylobacter jejuni: a comparative study with resonance Raman spectroscopy, Methods Enzymol. 437 (2008) 255–286, https://doi.org/10.1016/S0076-6879(07)37014-6.

[35] L.R. Milgrom, The Colours of Life, Oxford University Press, Oxford, 1997.

[36] B.R. Wood, D. McNaughton, Raman excitation wavelength investigation of single red blood cells in vivo, J. Raman Spectrosc. 33 (2002) 517–523, https://doi.org/10.1002/jrs.870.

[37] D. Perez-Guaita, K.M. Marzec, A. Hudson, C. Evans, T. Chernenko, C. Matthäus, M. Miljkovic, M. Diem, P. Heraud, J.S. Richards, D. Andrew, D.A. Anderson, C. Doerig, J. Garcia-Bustos, D. McNaughton, B.R. Wood, Parasites under the spotlight: applications of vibrational spectroscopy to malaria research, Chem. Rev. 118 (2018) 5330–5358, https://doi.org/10.1021/acs.chemrev.7b00661.

[38] K.M. Marzec, A. Rygula, B.R. Wood, S. Chlopicki, M. Baranska, High-resolution Raman imaging reveals spatial location of heme oxidation sites in single red blood cells of dried smears, J. Raman Spectrosc. 46 (2014) 76–83, https://doi.org/10.1002/jrs.4600.

[39] T.P. Wrobel, N. Piergies, E. Pieta, W. Kwiatek, C. Paluszkiewicz, M. Fornal, T. Grodzicki, Erythrocyte heme-oxygenation status indicated as a risk factor in prehypertension by Raman spectroscopy, Biochim. Biophys. Acta - Mol. Basis Dis. 1864 (2018) 3659–3663, https://doi.org/10.1016/j.bbadis.2018.07.006.

[40] P. Lemler, W.R. Premasiri, A. DelMonaco, L.D. Ziegler, NIR Raman spectra of whole human blood: effects of laser-induced and in vitro hemoglobin denaturation., Anal. Bioanal. Chem. 406 (2014) 193–200. https://doi.org/10.1007/s00216-013-7427-7.

[41] B.R. Wood, B. Tait, D. McNaughton, Micro-Raman characterisation of the R to T state transition of haemoglobin within a single living erythrocyte, Biochim. Biophys. Acta - Mol. Cell Res. 1539 (2001) 58–70, https://doi.org/10.1016/S0167-4889(01)00089-1.

[42] T.G. Spiro, T.C. Strekas, Resonance Raman spectra of heme proteins. Effects of oxidation and spin state, J. Am. Chem. Soc. 96 (1974) 338–345, https://doi.org/10.1021/ja00809a004.

[43] D. Morikis, P.M. Champion, B.A. Springer, K.D. Egeberg, S.G. Sligar, Resonance Raman studies of Iron spin and axial coordination in distal pocket mutants of ferric myoglobin*, J. Biol. Chem. 265 (1990) 12143–12145 (http://www.jbc.org/content/265/21/12143.full.pdf (accessed December 3, 2017)).

[44] B.R. Wood, B. Tait, D. McNaughton, Micro-Raman characterisation of the R to T state transition of haemoglobin within a single living erythrocyte, Biochim. Biophys. Acta - Mol. Cell Res. 1539 (2001) 58–70, https://doi.org/10.1016/S0167-4889(01)00089-1.

[45] M. Asghari-Khiavi, A. Mechler, K.R. Bambery, D. McNaughton, B.R. Wood, A resonance Raman spectroscopic investigation into the effects of fixation and dehydration on heme environment of hemoglobin, J. Raman Spectrosc. 40 (2009) 1668–1674, https://doi.org/10.1002/jrs.2317.

[46] J. Dybas, M.J. Bokamper, K.M. Marzec, P.J. Mak, Probing the structure-function relationship of hemoglobin in living human red blood cells, Spectrochim. Acta - Part A Mol. Biomol. Spectrosc. 239 (2020) 118530, https://doi.org/10.1016/j.saa.2020.118530.

[47] E.M. Welbourn, M.T. Wilson, A. Yusof, M.V. Metodiev, C.E. Cooper, The mechanism of formation, structure and physiological relevance of covalent hemoglobin attachment to the erythrocyte membrane, Free Radic. Biol. Med. 103 (2017) 95–106, https://doi.org/10.1016/j.freeradbiomed.2016.12.024.

[48] E. Lang, S.M. Qadri, F. Lang, Killing me softly – suicidal erythrocyte death, Int. J. Biochem. Cell Biol. 44 (2012) 1236–1243, https://doi.org/10.1016/j.biocel.2012.04.019.

[49] Y. Sugawara, Y. Hayashi, Y. Shigemasa, Y. Abe, I. Ohgushi, E. Ueno, F. Shimamoto, Molecular biosensing mechanisms in the spleen for the removal of aged and damaged red cells from the blood circulation, Sensors (Basel) 10 (2010) 7099–7121, https://doi.org/10.3390/s100807099.

[50] D.G. Kakhniashvili, L.A. Bulla, S.R. Goodman, The human erythrocyte proteome, Mol. Cell. Proteomics 3 (2004) 501–509, https://doi.org/10.1074/mcp.M300132-MCP200.

[51] J.E. Smith, Erythrocyte membrane: structure, function, and pathophysiology, Vet. Pathol. 24 (1987) 471–476 (http://www.ncbi.nlm.nih.gov/pubmed/3331858 (accessed March 6, 2016)).

[52] V. Pallotta, A. D'Alessandro, S. Rinalducci, L. Zolla, Native protein complexes in the cytoplasm of red blood cells, J. Proteome Res. 12 (2013) 3529–3546, https://doi.org/10.1021/pr400431b.

[53] R. Lu, W.-W. Li, A. Katzir, Y. Raichlin, B. Mizaikoff, H.-Q. Yu, Fourier transform infrared spectroscopy on external perturbations inducing secondary structure changes of hemoglobin, Analyst 141 (2016) 6061–6067, https://doi.org/10.1039/C6AN01477A.

[54] A. Blat, J. Dybas, M. Kaczmarska, K. Chrabaszcz, K. Bulat, R.B. Kostogrys, A. Cernescu, K. Malek, K.M. Marzec, An analysis of isolated and intact rbc membranes - a comparison of a semiquantitative approach by means of FTIR, nano-FTIR, and Raman spectroscopies, Anal. Chem. 91 (2019) 9867–9874, https://doi.org/10.1021/acs.analchem.9b01536.

[55] M.Z. Pacia, L. Mateuszuk, S. Chlopicki, M. Baranska, A. Kaczor, Biochemical changes of the endothelium in the murine model of NO-deficient hypertension, Analyst 140 (2015) 2178–2184, https://doi.org/10.1039/c4an01870b.

[56] A. Barth, Infrared spectroscopy of proteins, Biochim. Biophys. Acta Bioenerg. 1767 (2007) 1073–1101, https://doi.org/10.1016/j.bbabio.2007.06.004.

[57] A.A. Bunaciu, Ş. Fleschin, V.D. Hoang, H.Y. Aboul-Enein, Vibrational spectroscopy in body fluids analysis, Crit. Rev. Anal. Chem. 47 (2017) 67–75, https://doi.org/10.1080/10408347.2016.1209104.

[58] M. Mahato, P. Pal, T. Kamilya, R. Sarkar, A. Chaudhuri, G.B. Talapatra, Hemoglobin–silver interaction and bioconjugate formation: a spectroscopic study, J. Phys. Chem. B 114 (2010) 7062–7070, https://doi.org/10.1021/jp100188s.

[59] Y. Adigüzel, P.I. Haris, F. Severcan, Screening of proteins in cells and tissues by vibrational spectroscopy, Adv. Biomed. Spectrosc. 6 (2012) 53–108, https://doi.org/10.3233/978-1-61499-059-8-53.

[60] B. Shivu, S. Seshadri, J. Li, K.A. Oberg, V.N. Uversky, A.L. Fink, Distinct beta-sheet structure in protein aggregates determined by ATR-FTIR spectroscopy, Biochemistry 52 (2013) 5176–5183, https://doi.org/10.1021/bi400625v.

[61] D. Perez-Guaita, M. de Veij, K.M. Marzec, A.R.D. Almohammedi, D. McNaughton,

A.J. Hudson, B.R. Wood, Resonance Raman and UV–visible microscopy reveals that conditioning red blood cells with repeated doses of sodium dithionite increases haemoglobin oxygen uptake, ChemistrySelect 2 (2017) 3342–3346, https://doi.org/10.1002/slct.201700190.

[62] Y. Li, Y. Xiong, R. Wang, F. Tang, X. Wang, Blood banking-induced alteration of red blood cell oxygen release ability, Blood Transfus. 14 (2016) 238–244, https://doi.org/10.2450/2015.0055-15.

[63] U.J. Dumaswala, L. Zhuo, D.W. Jacobsen, S.K. Jain, K.A. Sukalski, Protein and lipid oxidation of banked human erythrocytes: role of glutathione, Free Radic. Biol. Med. 27 (1999) 1041–1049, https://doi.org/10.1016/S0891-5849(99)00149-5.

[64] Y. Xiong, Y. Xiong, Y. Wang, Z. Wang, A. Zhang, N. Zhao, D. Zhao, Z. Yu, Z. Wang, J. Yi, X. Luan, Inhibition of glutathione synthesis via decreased glucose metabolism in stored RBCs, Cell. Physiol. Biochem. 51 (2018) 2172–2184, https://doi.org/10.1159/000495864.

[65] M.E. Anderson, [70] Determination of Glutathione and Glutathione Disulfide in Biological Samples, in: 1985: pp. 548–555. https://doi.org/10.1016/S0076-6879(85)13073-9.

[66] H.J. Forman, H. Zhang, A. Rinna, Glutathione: overview of its protective roles, measurement, and biosynthesis, Mol. Asp. Med. 30 (2009) 1–12, https://doi.org/10.1016/j.mam.2008.08.006.

[67] B. Mannervik, Glutathione peroxidase, Methods Enzymol. 113 (1985) 490–495, https://doi.org/10.1016/S0076-6879(85)13063-6.

[68] S.K. Srivastava, E. Beutler, Glutathione metabolism of the erythrocyte. The enzymic cleavage of glutathione-haemoglobin preparations by glutathione reductase, Biochem. J. 119 (1970) 353–357. https://doi.org/10.1042/bj1190353.

[69] K. Kus, A. Kij, A. Zakrzewska, A. Jasztal, M. Stojak, M. Walczak, S. Chlopicki, Alterations in arginine and energy metabolism, structural and signalling lipids in metastatic breast cancer in mice detected in plasma by targeted metabolomics and lipidomics, Breast Cancer Res. 20 (2018) 148, https://doi.org/10.1186/s13058-018-1075-y.